Proceedings of the 17th World Congress
The International Federation of Automatic Control
Seoul, Korea, July 6-11, 2008

Reactive Navigation of a Mobile Robot in Unknown Environments

Guan-Chun Luh, Wei-Wen Liu, Huang-Kai, Lin

Mechanical Engineering Department, Tatung University,
Taipei City, Taiwan, Republic of China (Tel: 886-2-25925252 Ext:3410 Re-Ext: 806; e-mail:gluh@ttu.edu.tw)

Abstract: In this paper, a Reactive Immune Network (RIN) is proposed and employed for mobile robot navigation in unknown environments. Rather than building a detailed mathematical model of artificial immune systems, this study tries to explore the principle in an immune network focusing on its self-organization, adaptive learning capability, and immune feedback. In addition, an adaptive virtual target method is integrated to solve the local minima problem in navigation. Several trapping situations are adopted to evaluate the performance of the proposed architecture. Experimental results show that the mobile robot is capable of avoiding obstacles, escaping traps, and reaching the goal efficiently and effectively.

1. INTRODUCTION

Autonomous mobile robots have a wide range of applications in industries, hospitals, offices, and even the military, due to their superior mobility. In order to adapt the robot's behaviour to any complex, varying and unknown environment, path planning of robot behaviour plays an important role. The design goal for path planning is to enable a mobile robot to navigate safely and efficiently without collisions to a target position in an unknown and complex environment. The navigation strategies of mobile robots can be generally classified into two categories, global path planning and local reactive navigation. The later, employing some reactive strategies to perceive the environment based on the sensory information and path planning, is done online. The robot has to acquire a set of stimulus-action mechanisms through its sensory inputs, such as distance information from infrared sensors, visual information from cameras or processed data derived after appropriate fusion of numerous sensor outputs. The action taken by the robot is usually an alternation of steering angle and/or translation velocity to avoid collisions and reach the desired target.

Reactive behavior-based mobile robot responds to stimuli from the dynamic environment, and its behaviors are guided by local states of the world. Some researches demonstrated its robustness and flexibility against an unstructured world (Chang, 1996). However, a well-known drawback of reactive navigation is that the mobile robot suffers from local minima problems in that it uses only locally available environmental information without any previous memory. In other words, a robot may get trapped in front of an obstacle or wander indefinitely in a region whenever it navigates past obstacles toward a target position. Several trap escape algorithms, including the random walk method (Baraquand, and Latombe, 1990), the multi-potential field method (Chang, 1996), the tangent algorithm (Lee *et al.*, 1997), the wall-following method (Borenstein, and Koren,1989), the virtual obstacle scheme (Park and Lee, 2003), and the virtual target approach (Xu, 2000), have been proposed to solve the local minima problems.

In the last decade, it has been shown that the biologically inspired artificial immune system (AIS) has a great potential in the fields of machine learning, computer science and engineering (de Castro and Jonathan, 1999). Immunized systems consisting of agents (immune-related cells) may have adaptation and learning capabilities similar to artificial neural networks, except that they are based on dynamic cooperation of agents (Ishida, 1997). Accordingly, the artificial immune system can be expected to provide various feasible ideas for the navigation of mobile robots. Ishiguro *et al.* (1995) proposed a two-layer (situation-oriented and goal-oriented) immune network to behaviour control of autonomous mobile robots. Simulation results show that mobile robot can reach goal without colliding fixed or moving obstacles. Later, Lee *et al.* (2000) constructed obstacle-avoidance and goal-approach immune networks for the same purpose. Additionally, it shows the advantage of not falling into a local loop. Afterward, Vargas *et al.* (2003) developed an Immuno-Genetic Network for autonomous navigation. Some preliminary experiment on a real Khepera II robot demonstrated the feasibility of the network. Recently, Duan *et al.* (2004) proposed an immune algorithm for path planning of a car-like wheeled mobile robot. Simulations indicate that the algorithm can finish different tasks within shorter time. It should be noted that, however, all of the above researches did not consider solving the local minima problems.

2. HOW BIOLOGICAL IMMUNE SYSTEM WORKS

The immune system protects living organisms from foreign substances such as viruses, bacteria, and other parasites (called antigens). The body identifies invading antigens through two inter-related systems: the innate immune system and the adaptive immune system. The former is mediated mainly by phagocytes while the latter is mediated by lymphocytes. The adaptive immune system uses lymphocytes that can quickly change in order to destroy antigens that have

entered the bloodstream. Lymphocytes are responsible for the recognition and elimination of the antigens. They usually become active when there is some kind of interaction with an antigenic stimulus leading to the activation and proliferation of the lymphocytes. Two main types of lymphocytes, namely B-cells and T-cells, play a remarkable role in both immunities (*Roitt* et al., 1998). Both B-cell and T-cell express in their surfaces antigenic receptors highly specific to a given antigenic determinant. B-cells take part in the humoral immunity and secrete antibodies by the clonal proliferation while the latter takes part in cell-mediated immunity.

The immune system produces the diverse antibodies by recognizing the idiotype of the mutual receptors of the antigens between antigen and antibodies and between antibodies. The relation between antigens and antibodies and that amongst antibodies can be evaluated by the value of the affinity. In terms of affinities, the immune system self-regulates the production of antibodies and diverse antibodies. Affinity maturation occurs when the maturation rate of a B-cell clone increases in response to a match between the clone's antibody and an antigen. Those mutant cells are bound more tightly and stimulated to divide more rapidly.

Jerne (1973) has proposed the idiotypic network hypothesis (immune network hypothesis) based on mutual stimulation and suppression between antibodies. This hypothesis is modeled as a differential equation simulating the concentration of a set of lymphocytes. The concept of an immune network states that the network dynamically maintains the memory using feedback mechanisms within the network. The various species of lymphocytes are not isolated but communicate with each other through the interaction antibodies. Based on his speculation, several theories and mathematical models have been proposed. In this study, the dynamic equation proposed by Farmer *et al.* (1986) is employed as a reactive immune network to calculate the variation on the concentration of antibodies, as shown in the following equations:

$$\frac{dA_i(t)}{dt} = \left(\sum_{\ell=1}^{N_{Ab}} m_{i\ell}^{st} a_\ell(t) - \sum_{k=1}^{N_{Ab}} m_{ki}^{su} a_k(t) + m_i - k_i \right) a_i(t) \tag{1}$$

$$a_i(t) = \frac{1}{1+\exp(0.5 - A_i(t))}$$

where i, ℓ, k = 0, 1,$\cdots$, N_{Ab} are the subscripts to distinguish the antibody types and N_{Ab} is the number of antibodies. A_i and a_i are the stimulus and concentration of the ith antibody. m_{ij}^{st}, m_{ki}^{su} indicate the stimulative and suppressive affinity between the ith and the jth, kth antibodies, respectively. m_i denotes the affinity of antigen and antibody i, and k_i represents the natural death coefficient. Equation (1) is composed of four terms. The first term shows the stimulation, while the second term depicts the suppressive interaction between the antibodies. The third term is the stimulus from the antigen, and the final term is the natural extinction term, which indicates the dissipation tendency in the absence of any interaction. Equation (2) is a squashing function to ensure the stability of the concentration.

3. REACTIVE IMMUNE NETWORK

A reactive immune network inspired by the biological immune system for robot navigation (goal-reaching and obstacle-avoidance) is described in this section. It implies using a combination of both the prior behavior-based information and an on-line adaptation mechanism based on the features of the immune system. The architecture of the proposed navigation system is depicted in Fig. 1. The antigen's epitope is a situation detected by sensors and provides the information about the relationship between the current location and the obstacles, along with the target. The interpreter is regarded as a phagocyte and translates sensor data into perception. The antigen presentation proceeds from the information extraction to the perception translation. A paratope with a built-in robot's steering direction is regarded as an antibody and interacts with each other and with its environment. These antibodies/steering-directions are induced by recognition of the available antigens/detected-information. In should be noted that only one antibody with the highest concentration will be selected to act according to the immune network hypothesis.

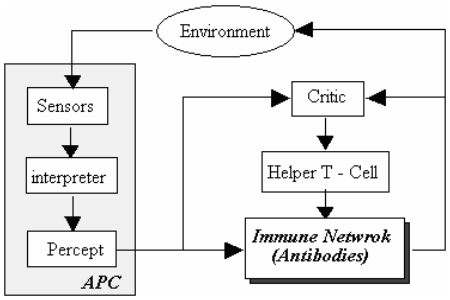

Fig. 1 The architecture of the immunized network system

In the proposed immune network, antibodies are defined as the steering directions of mobile robots as illustrated in Fig. 2,

$$Ab_i \equiv \theta_i = \frac{360°}{N_{Ab}}(i\text{-}1) \qquad i = 1,2,\cdots,N_{Ab} \tag{2}$$

where N_{Ab} is the number of antibodies/steering-directions and θ_i is the steering angle between the moving path and the head orientation of the mobile robot. Note that 0º$\leq \theta_i \leq$360º. In addition, the antigen represents the local environment surrounding the robot and its epitopes are a fusion data set containing the azimuth of the goal position θ_g, the distance between the obstacles and the jth sensor d_j, and the azimuth of sensor θ_{Sj}.

$$Ag_j \equiv \{\theta_g, d_j, \theta_{S_j}\} \qquad j = 1,2,\cdots,N_s \tag{3}$$

$$\theta_{S_j} \equiv \frac{360°}{N_S}(j\text{-}1) \qquad j = 1,2,\cdots,N_s \tag{4}$$

where N_s is the number of sensors equally spaced around the base plate of the mobile robot, $d_{\min} \leq d_j \leq d_{\max}$ and 0º $\leq \theta_{Sj} \leq$360º. Parameters $d_{\min}$ and $d_{\max}$ represent the nearest and longest distances measured by the range sensors, respectively. It should be noted that different antigens (local environments) might have identical epitopes (fusion information from range

sensors). There is no necessary relationship between N_{Ab} and N_s since they depend on the hardware of mobile robot.

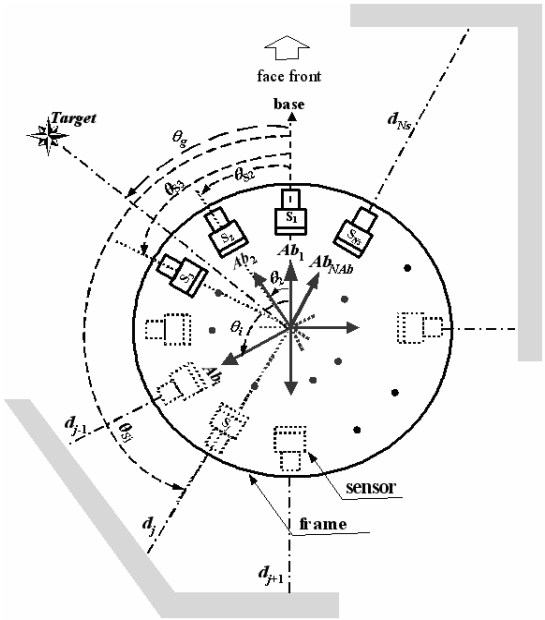

Fig. 2 Configuration of mobile robot, target and obstacles

The potential-field method is one of the most popular approaches employed to navigate the mobile robot within environments containing obstacles, since it is conceptually effective and easy to implement. The approach considers a virtual attractive force between the robot and the target as well as virtual repulsive forces between the robot and the obstacles. The resultant force on the robot is then used to decide the direction of its movements. In the proposed immune network, the resultant force on the robot is defined as m_i, the affinity value between the antigen/local environment and the *ith* antibody/steering angle,

$$m_i = w_1 F_{goal_i} + w_2 F_{obs_i} \qquad i = 1,2,\cdots,N_{Ab} \tag{5}$$

The weighing values w_1 and w_2 indicate the ratio between attractive and repulsive forces. Note that $0 \le w_1, w_2 \le 1$ and $w_1 + w_2 = 1$. The attractive force F_{goal_i} of the *i*th steering direction (*i.e.* the *i*th antibody) is defined as follows:

$$F_{goal_i} = \frac{1.0 + \cos(\theta_i - \theta_g)}{2.0}, \qquad i = 1,2,\cdots,N_{Ab} \tag{6}$$

Note that F_{goal_i} is normalized and $0 \le F_{goal_i} \le 1$. Obviously, the attractive force is at its maximal level ($F_{goal_i} = 1$) when the mobile robot goes straightforward to the target (*i.e.* $\theta_i = \theta_g$). On the contrary, it is minimized ($F_{goal_i} = 0$) if the robot's steering direction is the opposite of the goal.

The repulsive force for each moving direction (the *i*th antibody θ_i) is expressed as the following equation,

$$F_{obs_i} = \sum_{j=1}^{N_S} \alpha_{ij} \cdot \bar{d}_j \tag{7}$$

where $\alpha_{ij} = \exp(-N_s \times (1 - \delta_{ij}))$ with $\delta_{ij} = \dfrac{1 + \cos(\theta_i - \theta_{S_j})}{2}$.

Fig. 5 demonstrates the relationship between α_{ij} and δ_{ij}. α_{ij} indicates the weighting ratio for the *j*th sensor to steering angle θ_i while $\bar{d}_j$ represents the normalized distance between the *j*th sensor and the obstacles. Coefficient δ_{ij} expresses influence and importance of each sensor at different locations. It shows that the information derived from the sensor closest to the steering direction is much more important due to its biggest δ_{ij} value. Kubota *et al.* [44] have proposed a similar 'delta rule' to evaluate the weighting of each sensor.

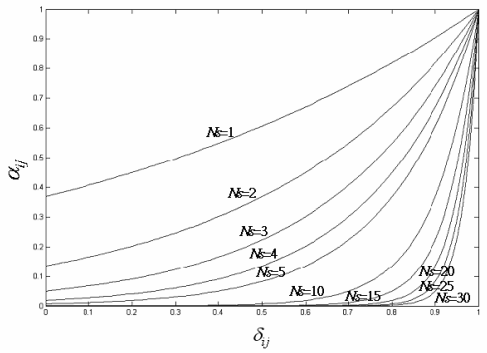

Fig. 3 Relation between α_{ij} and δ_{ij}

The normalized obstacle distance for each sensor $\bar{d}_j$ is fuzzified using the fuzzy set definitions. The mapping from the fuzzy subspace to the TSK model is represented as three fuzzy if-then rules in the form of sensor too.

IF d_j is ***s*** THEN $y=L_1$
IF d_j is ***m*** THEN $y=L_2$ (8)
IF d_j is ***d*** THEN $y=L_3$

where L_1, L_2, and L_3 are defined as 0.25, 0.5 and 1.0, respectively. The input variable of each rule is the detected distance d_j of the *j*th sensor. The antecedent part of each rule has one of the three labels, namely, ***s*** (safe), ***m*** (medium), and ***d*** (danger). Consequently, the total output of the fuzzy model is given by the equation below,

$$\bar{d}_j = \frac{\mu_{safe}(d) \cdot L_1 + \mu_{medium}(d) \cdot L_2 + \mu_{danger}(d) \cdot L_3}{\mu_{safe}(d) + \mu_{medium}(d) + \mu_{danger}(d)} \tag{9}$$

where $\mu_{safe}(d)$, $\mu_{medium}(d)$, $\mu_{danger}(d)$, represent the matching degree of the corresponding rule. The inputs to the TSK model are crisp numbers; therefore, the degree of the input matches its rule is and computed using the "min operator". Fig. 6 illustrates the membership function and labels for measured distance d_j.

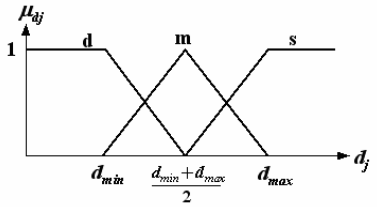

Fig. 4 Membership function

As to the stimulative-suppressive interaction between the antibodies/steering-directions are derived from equation (1) as follows,

$$\begin{aligned}\frac{dA_i(t)}{dt} &= \left(\sum_{\ell=1}^{N_{Ab}} m_{i\ell}^{st} a_\ell(t) - \sum_{k=1}^{N_{Ab}} m_{ki}^{su} a_k(t) + m_i - k_i\right) a_i(t) \\ &= \left[\left(m_{i1}^{st} a_1(t) + m_{i2}^{st} a_2(t) + \cdots + m_{iN_{Ab}}^{st} a_{N_{Ab}}(t)\right) - \left(m_{1i}^{su} a_1(t) + m_{2i}^{su} a_2(t) + \cdots + m_{N_{Ab}i}^{su} a_{N_{Ab}}(t)\right) + m_i - k_i\right] a_i(t) \\ &= \left[\left(m_{i1}^{st} - m_{1i}^{su}\right) a_1(t) + \left(m_{i2}^{st} - m_{2i}^{su}\right) a_2(t) + \cdots + \left(m_{iN_{Ab}}^{st} - m_{N_{Ab}i}^{su}\right) a_{N_{Ab}}(t) + m_i - k_i\right] a_i(t) \\ &= \left[m_{i1}^{ss} a_1(t) + m_{i2}^{ss} a_2(t) + \cdots + m_{iN_{Ab}}^{ss} a_{N_{Ab}}(t) + m_i - k_i\right] a_i(t) \\ &= \left(\sum_{\ell=1}^{N_{Ab}} m_{i\ell}^{ss} a_\ell(t) + m_i - k_i\right) a_i(t) \end{aligned} \quad (10)$$

and the stimulative-suppressive affinity $m_{i\ell}^{ss}$ between the ith and jth antibody/steering-angle is defined as

$$m_{i\ell}^{ss} = m_{i\ell}^{st} - m_{\ell i}^{su} = \cos(\theta_i - \theta_\ell) = \cos(\Delta\theta_{i\ell}), \qquad i, \ell = 1,2,\cdots, N_{Ab}$$

Obviously, stimulative-suppressive effect is positive ($m_{i\ell}^{ss} > 0$) if -90° < $\Delta\theta_{i\ell}$ < 90°. On the contrary, negative stimulative-suppressive effect exists between two antibodies if their difference of steering angles are greater than 90° or less than -90°. In addition, there is no any net effect between orthogonal antibodies (*i.e.* $\Delta\theta_{i\ell}$ = ±90°). The immune system responses to the specified winning situation that has the maximum concentration among the antibodies be trigged by comparing the currently perceived situations (trigged antibodies). In other words, antibody with the highest concentration is selected to activate its corresponding behavior to the world. Therefore, mobile robot moves a step along the direction of the chosen steering angle/antibody.

4. LOCAL MINIMUM RECOVERY

As mentioned in the previous section, one problem inherent in the potential-field method is the possibility for the robot to get trapped in a local minima situation. Traps can be created by a variety of obstacle configurations. The key issue to the local minima problems is the detection of the local minima situation during the robot's traversal. In this study, the comparison between the robot-to-target direction θ_g and the instantaneous direction of travel θ_i was utilized to detect if the robot got trapped. The robot is very likely to get trapped and starts to move away from the goal if the robot's direction of travel is more than 90º off-target (*i.e.* $|\theta_i - \theta_g| > 90º$). In this study, an adaptive virtual target method is developed and integrated with the reactive immune network to guide the robot out of the trap.

In immunology, the T-cell plays a remarkable key role in distinguishing a "self" from other "non-self" antigens. The Helper-T cells work primarily by secreting substances to constitute powerful chemical messengers to promote cellular growth, activation and regulation. Simulating the biological immune system, this material can either stimulate or suppress the promotion of antibodies/steering-directions depending on whether the antigen is non-self or self (trapped in local minima or not). Different from the virtual target method proposed in [10], an additional virtual robot-to-target angle θ_v (analogous to the interleukine secreted by T-cells) is added to the goal angle θ_g whenever the trap condition (*i.e.* $|\theta_i - \theta_g| > 90º$) is satisfied,

$$\theta_g(k+1) = \theta_g(k) + \theta_v(k) \quad (11)$$

with

$$\begin{cases} \theta_v(k) = \theta_v(k-1) \pm \Delta\theta_g & \text{if } |\theta_i(k) - \theta_g(k)| \geq 90° \text{ and } \theta_v(k-1) = 0 \\ \theta_v(k) = \theta_v(k-1) + sign(\theta_v(k-1)) \cdot \Delta\theta_g & \text{if } |\theta_i(k) - \theta_g(k)| \geq 90° \text{ and } \theta_v(k-1) \neq 0 \\ \theta_v(k) = \max\{0, \theta_v(k-1) - sign(\theta_v(k-1)) \cdot \theta_c(k-1)\} & \text{if } |\theta_i(k) - \theta_g(k)| < 90° \text{ and } \theta_v(k-1) \geq 0 \\ \theta_v(k) = \min\{0, \theta_v(k-1) - sign(\theta_v(k-1)) \cdot \theta_c(k-1)\} & \text{if } |\theta_i(k) - \theta_g(k)| < 90° \text{ and } \theta_v(k-1) < 0 \end{cases}$$

where $\Delta\theta_g = \theta_g(k) - \theta_g(k\text{-}1)$ and $\theta_c(k) = \theta_c(k\text{-}1) + \lambda$

Parameters k-1, k, and k+1 represent the previous state, the current state and the future state, respectively. Symbol "±" indicates that the location of the virtual target can be randomly switched to either the right (*i.e.* "+") or the left (*i.e.* "–") side of the mobile robot so that the robot has a higher probability of escaping from the local minima in either direction. λ is an adjustable decay angle. The bigger the value is, the faster the location of virtual target converges to that of the true one and the easier it is for the robot to get trapped in the local minima again. In this study, λ is determined after multiple simulation runs and set to 0.2. The incremental virtual angle $\theta_v(k)$ in the proposed scheme is state dependent and self-adjustable according to the robot's current state and the action it took previously. This provides powerful and effective trap-escaping capability compared to virtual target method, which keeps θ_v a constant value. θ_c is a converging angle and its initial value is 0.

For carrying out the necessary simulation and validating the efficacy of the proposed methodology, a computer program was developed using C++ language with graphical user interface. The simulation environment contains a robot and obstacle constructed by numerous square blocks 10cm in length. The environmental condition adopted in simulation is a 300cm×300cm grid. The size of the simulated robot is a circle with 10cm diameter. Fig. 5 elucidates and demonstrates the performance of the proposed strategy for the robot to escape from a recursive U-trap situation, which may make the virtual target switching strategy [10] ineffective as Chatterjee and Matsuno [12] suggested.

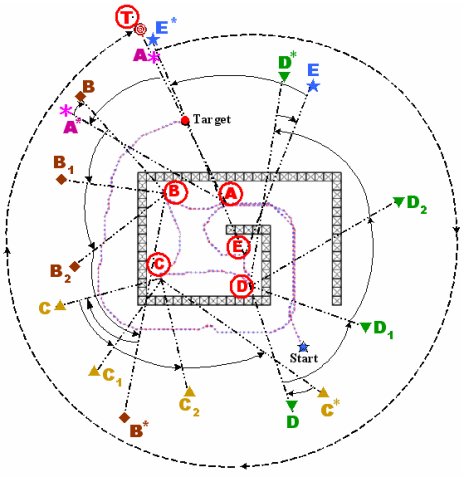

Fig. 5 Robot path and state of the indices along the trajectory

The robot first enters a U-shaped obstacle and is attracted to the target due to the target's reaching behavior until it reaches the critical point Ⓐ. Clearly, the azimuth of goal θ_g is kept the same during this stage; however, the distance between the robot and the target is decreased quickly. The detection of the trap possibility because of the abrupt change of target orientation at location Ⓐ (θ_g) makes the target shift to a virtual position A^* (θ_g-$\Delta\theta_g$). $\Delta\theta_g$ is defined as 45° is this study. Note that the switch-to-left or the switch-to-right of the virtual target (*i.e.*, minus or plus $\Delta\theta_g$) is selected randomly. On the way Ⓐ→Ⓑ, $\Delta\theta_g$ is decreased gradually according to equation (8) until a new local minimal is found at location Ⓑ. Again, the location of virtual target switches from A^* to B^*. Fig. 9 and Fig. 10 show that there is a successive virtual target switching $A^*\rightarrow B_1\rightarrow B_2\rightarrow B^*$ when the robot moves around the left upper corner where it is tracked in a trap (to satisfy condition $|\theta_i - \theta_g| > 90°$) three times. After passing through the critical point Ⓑ, the robot keeps approaching the virtual target until reaching the third critical point Ⓒ. Concurrently, the associated orientation of the virtual target is decreased from B^* to C. Once more, it takes three times for the robot to escape from the trap situation in the left lower corner on the path Ⓒ→Ⓓ (orientation of the virtual target $C\rightarrow C_1\rightarrow C_2\rightarrow C^*\rightarrow D$). Similar navigation procedures take place on the way Ⓓ→Ⓔ (orientation of virtual target $D\rightarrow D_1\rightarrow D_2\rightarrow D^*\rightarrow E\rightarrow E^*$). After escaping from the recursive U-shaped trap, the mobile robot revolves in a circle and finally reaches target Ⓣ without any trapping situations (azimuth of virtual target θ_g decreases gradually from E^* to T illustrated with a dashed line). The derived trajectory illustrated in Fig. 9 is quite similar to the results derived by Chatterjee and Matsuno [12]. Fig. 6 illustrates the other possible trajectory to escape the same trap situation due to the random choice of the "plus" or "minus" robot-to-target angle $\Delta\theta_g$, as shown in equation (8). Obviously, the mechanism for virtual target switching to the right or to the left (*i.e.*, $\pm\Delta\theta_g$) increases the diversity and possibility of the robot's escaping from the local minima problem.

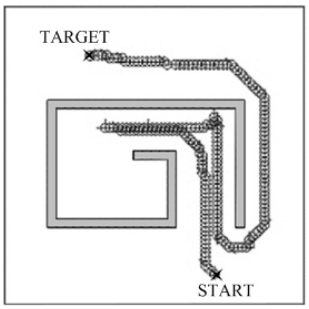

Fig. 6 The other possible escape trajectory

5. EXPERIMENTAL RESULTS

Numerous experiments were implemented to evaluate the performance in real application. Fig. 7 shows the mobile robot (with omni-directional wheel) used. It's dimension is 416*mm*×363.7*mm*×670*mm*. The robot installed with 8 ultrasonic sensors, two web-cams, and a laser range finder. Figs.8-11 demonstrate the pictures of the robot navigate in two "U" shape obstacles (with different length and width: 160*mm*×320*mm*, and 300*mm*×100*mm*) and their corresponding trajectories, respectively. All these figures show that the mobile robot is capable of navigating to the goal and escaping from local minimum traps employing the proposed reactive immune network. Note that mobile robot can approach target from both sides randomly as described in previous section.

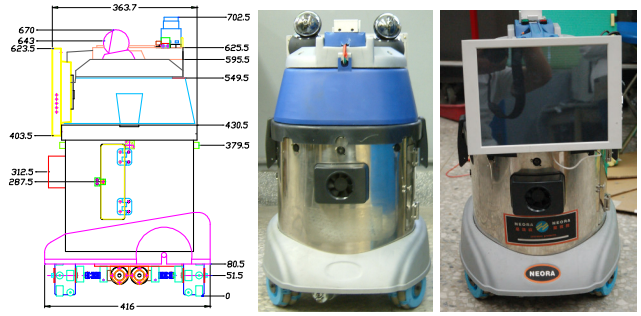

Fig. 7 Dimension and pictures of the mobile robot

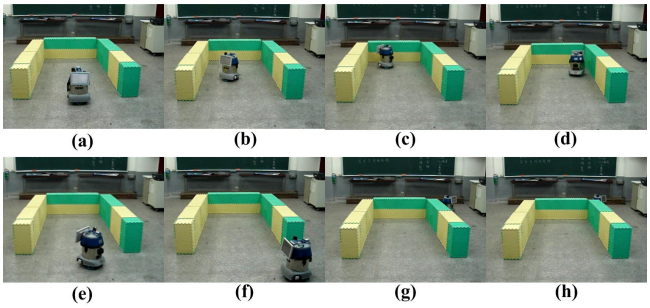

Fig. 8 Navigation of robot in 160mm×320mm "U" obstacle

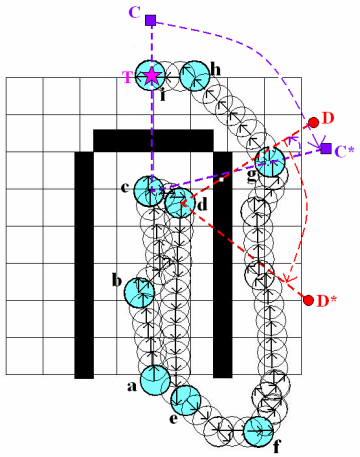

Fig. 9 Trajectories of robot in 160mm×320mm "U" obstacle

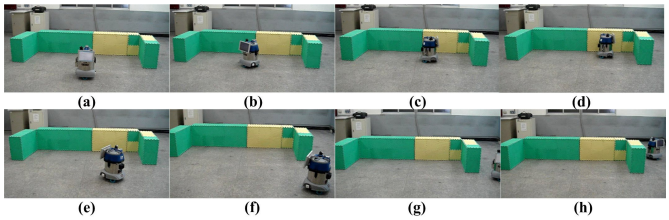

Fig. 10 Navigation of robot in 300mm×100mm "U" obstacle

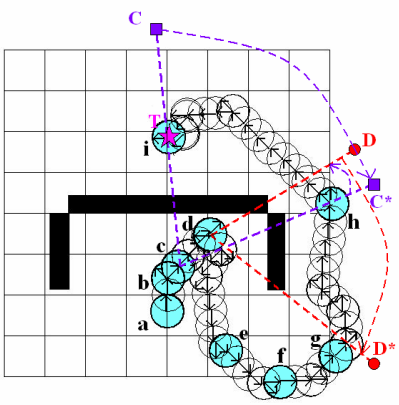

Fig. 11 Trajectories of robot in 300mm×100mm "U" obstacle

Figs. 12, 13 illustrate the pictures of the robot navigate in a "sequential-U" shape obstacle (400*mm*×190*mm* with a 90*mm* bar in middle) and its corresponding trajectory, respectively. Apparently, the mobile robot is able to navigate easily employing the proposed reactive immune network.

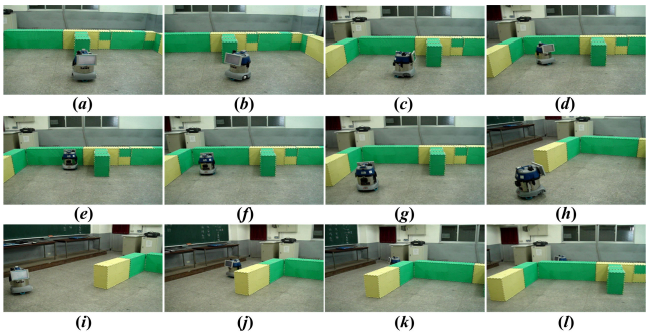

Fig.12 Navigation of robot in "sequential-U" shape obstacle

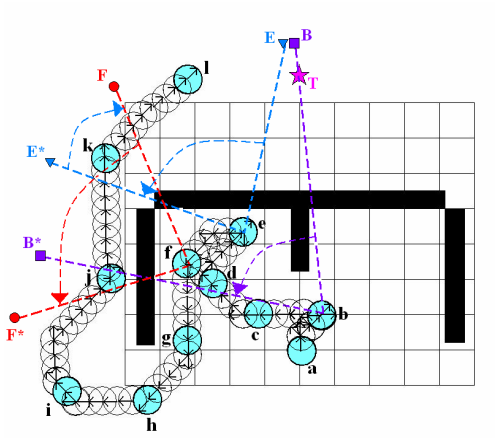

Fig. 13 Trajectories in "sequential-U" shape obstacle

5. CONCLUSIONS

A reactive immune network inspired by the biological immune system is proposed for mobile robot navigation. In addition, an adaptive virtual target method is integrated to solve the local minima problem. Several "U" shape trap environments are employed to evaluate the performance of the proposed methodology. Experimental results validate the flexibility, efficiency and effectiveness of the robot navigation architecture, especially the solution of the local minima problem.

RFERENCES

Baraquand, J. and J.C. Latombe (1990). A Monte-Carlo algorithm for path planning with many degrees of freedom. In: *Proceedings of the IEEE International Conference on Robotics and Automation*, 1712-1717.

Borenstein, J. and Y. Koren (1989). Real-time obstacle avoidance for fast mobile robots, *IEEE Transaction on System, Man and Cybernetics*, **9**, 1179-1197.

Chang, H. (1996). A new technique to handle local minima for imperfect potential field based motion planning, in: *Proceedings of the IEEE International Conference on Robotics and Automation*, 108-112.

de Castro, L.N. and T. Jonathan (1999). *Artificial immune systems: A new Computational Intelligence Approach*, Springer-Verlag.

Duan, Q.J., R.X. Wang, H.S. Feng and L.G. Wang (2004). An immunity algorithm for path planning of the autonomous mobile robot, In: *IEEE 8th International Multitopic Conference*, 69-73.

Farmer, J.D., N.H. Packard and A.S. Perelson (1986). The immune system adaptation, and machine learning. *Physica*, **22-D**, 184- 204.

Ishiguro, A., Y. Watanabe and Y. Uchikawa (1995). An immunological approach to dynamic behavior control for autonomous mobile robots, In: *IEEE/RSJ International Conference on Intelligent Robots and Systems*, 495-500.

Ishida, Y. (1997). The immune system as a prototype of autonomous decentralized systems: an overview, In: *Proceedings of Third International Symposium on autonomous decentralized systems*, 85-92.

Jerne, N.K. (1973). *The immune system*, Scientific American, **229**, 52-60.

Lee, D.-J., M.-J. Lee, Y.-K. Choi, and S. Kim (2000). Design of autonomous mobile robot action selector based on a learning artificial immune network structure, In: *Proceedings of the fifth Symposium on Artificial Life and Robotics*, 116-119.

Lee, S., T.M. Adams, and Ryoo, B.-Y. (1997). A fuzzy navigation system for mobile construction robots, *Automation in Construction*, **6**, 97-107.

Park, M.G. and M.C. Lee (2003). Artificial potential field based path planning for mobile robots using a virtual obstacle concept, In: *Proceedings of the IEEE/ASME International Conference on Advanced Intelligent Mechatronics*, 735-740.

Roitt, I., J. Brostoff, and D.K. Male (1998). *Immunology*, 5th ed. Mosby International Limited.

Vargas, P.A., L.N. de Castro, R. Michelan, and F.J. Von Zuben (2003). Implementation of an Immuno-Gentic Network on a Real Khepera II Robot, In: *IEEE Congress on Evolutionary Computation*, 420-426.

Xu, W.L. (2000). A virtual target approach for resolving the limit cycle problem in navigation of a fuzzy behaviour-based mobile robot. *Robotics and Autonomous Systems*, **30**, 315-324.